Proceedings 10th NUMGE 2023
10th European Conference on Numerical Methods in Geotechnical Engineering
Zdravkovic L, Kontoe S, Taborda DMG, Tsiampousi A (eds)

https://doi.org/10.53243/NUMGE2023-62

A computationally efficient consistent tangent operator for explicit stress integration techniques

L. Monforte[1,2], M. Rouainia[1]

[1]*Department of Engineering, Newcastle University, Newcastle, UK*
[2]*Centre Internacional de Mètodes Numèrics en Enginyeria (CIMNE), Barcelona, SPAIN*

ABSTRACT: The robustness, accuracy and efficiency of finite element simulations rely to a large extent on the numerical integration scheme of the constitutive model. The main advantage of implicit stress integration techniques over explicit methods is that expressions for the consistent tangent operator can be proposed, which preserve the quadratic rate of convergence of the Newton-Raphson method used to solve the global problem. In this work, a new expression for the consistent tangent operator for explicit stress integration techniques of small strain elasto-plastic models is proposed. The newly developed consistent tangent operator is assessed in several numerical analyses, showing a good performance and quadratic convergence rate in the iterative solution of the global problem.

Keywords: Stress integration; consistent tangent operator; elasto-plasticity; Runge-Kutta; Linearization.

1 INTRODUCTION

Stress integration techniques can be either explicit (Sloan et al., 2001) or implicit (Simo, 1998). Each class of methods has different properties in terms of efficiency, accuracy and robustness. Implicit methods are sometimes preferred due to their excellent convergence and unconditional numerical stability but more importantly because expressions for the so-called consistent stiffness matrix have been proposed. The word consistent is used to denote that the stiffness matrix used in the iterative solver of the global problem is congruous with the stress integration technique and is different from the continuous stiffness matrix. The use of the consistent tangent matrix guarantees a quadratic rate of asymptotic convergence of the Newton-Raphson method when used to solve the global problem, thus effectively representing a potential time saving in the iterative solver of the global problem.

Due to the increasing level of acceptance of implicit stress integration techniques (Simo and Hughes, 1998), expressions for the consistent stiffness matrix for various constitutive models have been proposed (Borja, 1989; Rouainia and Muir Wood, 2001), even considering adaptive substepping (Pérez-Foguet et al., 2001) or Implicit/Explicit (Implex) techniques (Oliver et al., 2008).

Runge-Kutta based explicit stress integration techniques (Sloan et al., 2001) are sometimes preferred due to their high-order accuracy, no requirements for the computation of second order derivatives of the yield surface and plastic potential, and straightforward implementation of adaptive-substepping schemes with error control (Lloret-Cabot and Sheng, 2022). However, the resulting explicit stress integration algorithm is far more complex compared to its implicit counterpart as it is generally recommended to correct yield surface drift and locate the yield surface intersection with the elastic trial stress path.

Explicit stress integration techniques also have the disadvantage that an expression for the consistent tangent matrix has not yet been proposed; therefore, the quadratic convergence of the Newton-Raphson iteration used to solve the global problem is not guaranteed. Consequently, higher-order accurate stress calculations need a high number of iterations to solve the global problem.

In this work, a new expression for the consistent tangent operator for explicit stress integration techniques of small strain elasto-plastic models is proposed. Due space limitations, here we report the expression of the consistent tangent operator for the case that the strain increment results in either the elastic or elasto-plastic regime. There is no difficulty in extending the expression to more complex explicit stress integration schemes (Sloan et al., 2001), including substepping and correction of yield surface drift (Monforte and Rouainia, 2023). Various numerical examples are performed to show the good performance of the developed consistent tangent operator and the quadratic rate of convergence in the iterative solution of the global problem.

2 CONTINUUM ELASTO-PLASTIC MODELS

An elasto-plastic model at small strain can be expressed as:

$$\begin{cases} \dot{\boldsymbol{\epsilon}} = \dot{\boldsymbol{\epsilon}}^e + \dot{\boldsymbol{\epsilon}}^p \\ \dot{\boldsymbol{\epsilon}}^p = \dot{\gamma}\frac{\partial g(\boldsymbol{\sigma},\ \boldsymbol{z})}{\partial \boldsymbol{\sigma}} \\ \dot{\boldsymbol{z}} = \dot{\gamma}\,\boldsymbol{h}(\boldsymbol{\sigma},\boldsymbol{z}) \\ \dot{\boldsymbol{\sigma}} = \boldsymbol{D} : \dot{\boldsymbol{\epsilon}}^e \end{cases} \tag{1}$$

where $\dot{\boldsymbol{\epsilon}}$, $\dot{\boldsymbol{\epsilon}}^e$ and $\dot{\boldsymbol{\epsilon}}^p$ are the temporal derivative of the total, elastic and plastic strain tensors, $\boldsymbol{\sigma}$ is the effective Cauchy stress tensor, $\boldsymbol{D} = \boldsymbol{D}(\boldsymbol{\sigma})$ is the fourth order elastic stiffness tensor, which may depend on stresses, $\boldsymbol{z}$ contains a set of n_z internal plastic variables, $g(\boldsymbol{\sigma},\ \boldsymbol{z})$ is the plastic potential, $\boldsymbol{h}(\boldsymbol{\sigma},\boldsymbol{z})$ is a vector of size n_z controlling the evolution of internal plastic variables, and $\dot{\gamma}$ is the plastic multiplier.

The problem has also to fulfill the Kuhn-Tucker and consistency conditions:

$$\begin{cases} f(\boldsymbol{\sigma},\boldsymbol{z}) \le 0 \\ \dot{\gamma} \ge 0 \\ \dot{\gamma}\, f(\boldsymbol{\sigma},\boldsymbol{z}) = 0 \\ \dot{\gamma}\ \dot{f}\ (\boldsymbol{\sigma},\boldsymbol{z}) = 0 \end{cases} \tag{2}$$

where $f(\boldsymbol{\sigma},\boldsymbol{z})$ is the yield surface.

In the elasto-plastic regime, the temporal derivative of the Cauchy stress tensor and internal variables may be related to the temporal derivative of the stress tensor through:

$$\dot{\boldsymbol{\sigma}} = \left(\boldsymbol{D} - \frac{\boldsymbol{D}:\frac{\partial g}{\partial \boldsymbol{\sigma}}\otimes\frac{\partial f}{\partial \boldsymbol{\sigma}}:\boldsymbol{D}}{H + \frac{\partial g}{\partial \boldsymbol{\sigma}}:\boldsymbol{D}:\frac{\partial f}{\partial \boldsymbol{\sigma}}}\right):\dot{\boldsymbol{\epsilon}} \tag{3}$$

$$\dot{\boldsymbol{z}} = h(\boldsymbol{\sigma},\boldsymbol{z})\left(\frac{\frac{\partial f}{\partial \boldsymbol{\sigma}}:\boldsymbol{D}}{H + \frac{\partial g}{\partial \boldsymbol{\sigma}}:\boldsymbol{D}:\frac{\partial f}{\partial \boldsymbol{\sigma}}}\right):\dot{\boldsymbol{\epsilon}} \tag{4}$$

where the hardening modulus is defined as $H = -\frac{\partial f}{\partial \dot{\gamma}}$.

In the elastic regime the plastic multiplier is null and consequently:

$$\dot{\boldsymbol{\sigma}} = \boldsymbol{D}:\dot{\boldsymbol{\epsilon}} \tag{5}$$

$$\dot{\boldsymbol{z}} = \boldsymbol{0} \tag{6}$$

Using Voigt's notation, we can express the temporal derivative of a generalized stress, $\boldsymbol{\Sigma}$, in terms of the temporal derivative of the strains as:

$$\dot{\boldsymbol{\Sigma}} = \begin{bmatrix}\dot{\boldsymbol{\sigma}} \\ \dot{\boldsymbol{z}}\end{bmatrix} = \boldsymbol{\Psi}(\boldsymbol{\Sigma}):\dot{\boldsymbol{\epsilon}} \tag{7}$$

where $\boldsymbol{\Psi}$ is a generalized stiffness matrix whose definition is different during the elastic or elasto-plastic regime. Based on Equations (3) and (4), the generalized stiffness matrix in the elasto-plastic regime is expressed as:

$$\boldsymbol{\Psi}_{EP}(\boldsymbol{\Sigma}) = \begin{bmatrix} \boldsymbol{D} - \frac{\boldsymbol{D}\cdot\frac{\partial g}{\partial \boldsymbol{\sigma}}\cdot\left(\frac{\partial f}{\partial \boldsymbol{\sigma}}\right)^T\cdot\boldsymbol{D}}{H+\left(\frac{\partial g}{\partial \boldsymbol{\sigma}}\right)^T\cdot\boldsymbol{D}\cdot\frac{\partial f}{\partial \boldsymbol{\sigma}}} \\ h(\boldsymbol{\sigma},\boldsymbol{z})\cdot\left(\frac{\left(\frac{\partial f}{\partial \boldsymbol{\sigma}}\right)^T\cdot\boldsymbol{D}}{H+\left(\frac{\partial g}{\partial \boldsymbol{\sigma}}\right)^T\cdot\boldsymbol{D}\cdot\frac{\partial f}{\partial \boldsymbol{\sigma}}}\right) \end{bmatrix} \tag{8}$$

whereas in the elastic regime:

$$\boldsymbol{\Psi}_E(\boldsymbol{\Sigma}) = \begin{pmatrix} \boldsymbol{D} \\ \boldsymbol{0}_{n_z\times 6}\end{pmatrix} \tag{9}$$

where $\boldsymbol{0}_{n_z\times 6}$ is a zero matrix of size $n_z \times 6$.

3 EXPLICIT STRESS INTEGRATION SCHEME

The stress integration algorithm for implicit techniques is quite straightforward: first a trial elastic is computed and if the stress state lays outside of the current yield surface, the consistency condition is enforced. The computation of the trial stress state is generally explicit, and a non-linear system of equations has to be solved if a plastic correction is required. On the contrary, explicit algorithms are far more laborious to code.

In the present work, a modified version of the Sloan et al. (2001) algorithm is adopted. As in the original proposal four different cases are considered which are treated differently: (i) all the strain increment results in elastic straining, (ii) all the strain increment occurs in elasto-plastic regime, (iii) plastic flow is preceded by elastic loading and (iv) plastic straining is preceded by elastic unloading. In the last two cases, the intersection between the stress path and the yield surface is located so that part of the deformation is integrated with the elastic update equations and the rest with the elasto-plastic equations. Also, in situations in which the final stress state is elasto-plastic, routines to correct yield surface drift are employed. Differently from the original proposal of Sloan et al. (2001), in this work adaptive substepping is not considered, but substepping can be included (Monforte and Rouainia, 2023).

As stated, in the present work only the linearization of a single strain increment in either the elastic or elasto-plastic regime increment is presented. As such, only a detailed description of the integration of a single strain increment is described. Full details of the Gauss point algorithm can be found elsewhere (Sloan et al., 2001; Monforte and Rouainia, 2023).

Given an increment of strain $\Delta\boldsymbol{\epsilon}_{n+1}$ and an initial generalized stress $\boldsymbol{\Sigma}_n$, the stress state at the new configuration is obtained by integrating Equation (7) between t_n and t_{n+1}. Without loss of generality, we can assume that the temporal variation of $\boldsymbol{\epsilon}$ in the interval is constant (Hiley and Rouainia, 2008), so the strain tensor increases linearly with time. This way, for $t_n < t < t_{n+1}$:

$$\dot{\boldsymbol{\epsilon}} = \frac{\Delta\boldsymbol{\epsilon}_{n+1}}{\Delta t_{\mathrm{n+1}}} \tag{10}$$

Then, Equation (7) becomes:

$$\dot{\boldsymbol{\Sigma}} = \boldsymbol{\Psi}(\boldsymbol{\Sigma}) \cdot \frac{\Delta\boldsymbol{\epsilon}_{n+1}}{\Delta t_{\mathrm{n+1}}} = \frac{1}{\Delta t_{\mathrm{n+1}}} \mathbf{F}(\boldsymbol{\Sigma}, \Delta\boldsymbol{\epsilon}_{n+1}) \tag{11}$$

where the function $\mathbf{F}(\boldsymbol{\Sigma}, \Delta\boldsymbol{\epsilon}_{n+1}) = \boldsymbol{\Psi}(\boldsymbol{\Sigma}) \cdot \Delta\boldsymbol{\epsilon}_{n+1}$ has been defined, which will facilitate further developments. As in the case of $\boldsymbol{\Psi}$, the appropriate elastic or elasto-plastic definition of $\mathbf{F}$ is used for each type of loading.

The explicit numerical integration of Equation (11) with a Runge-Kutta method may be expressed as:

$$\boldsymbol{\Sigma}^{n+1} = \boldsymbol{\Sigma}^{n} + \Delta t_{\mathrm{n+1}} \sum_{i=1}^{n} b_i \, \mathbf{k}_{\mathrm{i}}^{\star} \tag{12}$$

Or alternatively:

$$\boldsymbol{\Sigma}^{n+1} = \boldsymbol{\Sigma}^{n} + \sum_{i=1}^{n_s} b_i \, \mathbf{k}_i \tag{13}$$

where n_s is the number of stages of the Runge-Kutta method, b_i are coefficients of the integration method and:

$$\mathbf{k}_i = \boldsymbol{F}\left(\boldsymbol{\Sigma}^{n} + \sum_{j=1}^{j<i} a_{ij} \, \mathbf{k}_j, \; \Delta\boldsymbol{\epsilon}_{n+1}\right) \tag{14}$$

where a_{ij} are coefficients of the integration method.

4 CONSISTENT TANGENT OPERATOR

Equations (13) and (14) define the update equations for a single strain increment in either the elastic or elasto-plastic regime. This section is devoted to obtaining a consistent tangent operator for this case. The consistent tangent operator may be defined as (Simo, 1998; Rouainia and Muir Wood, 2001; Armero and Pérez-Foguet, 2002):

$$\boldsymbol{H}^{n+1} = \frac{\mathrm{d}\,\boldsymbol{\sigma}_{n+1}}{\mathrm{d}\,\Delta\boldsymbol{\epsilon}_{n+1}} \tag{15}$$

that is, the total derivative of the actualized Cauchy stress tensor, $\boldsymbol{\sigma}_{n+1}$, with respect to the strain increment, $\Delta\boldsymbol{\epsilon}_{n+1}$.

Let us note that the consistent tangent operator may be obtained from the generalized stress, $\boldsymbol{\Sigma}_{n+1}$, through:

$$\boldsymbol{H}^{n+1} = \frac{\mathrm{d}\,\boldsymbol{\sigma}_{n+1}}{\mathrm{d}\,\Delta\boldsymbol{\epsilon}_{n+1}} = \boldsymbol{P} \cdot \frac{\mathrm{d}\,\boldsymbol{\Sigma}_{n+1}}{\mathrm{d}\,\Delta\boldsymbol{\epsilon}_{n+1}} \tag{16}$$

where $\boldsymbol{P} = \left[\mathbf{1}_6, \mathbf{0}_{6\times n_z}\right]$ is a projection matrix, and $\mathbf{1}_6$ is an identity of size 6.

By introducing the generalized stress at t_{n+1}, Equation (13), in the definition of the consistent tangent matrix, Equation (16) becomes:

$$\boldsymbol{H}^{n+1} = \boldsymbol{P} \cdot \frac{\mathrm{d}}{\mathrm{d}\,\Delta\boldsymbol{\epsilon}_{n+1}} \left(\boldsymbol{\Sigma}^{n} + \sum_{i=1}^{n_s} b_i \, \mathbf{k}_i\right) \tag{17}$$

The derivative of the generalized stress at time t_n with respect to the increment of strain is null, thus Equation (17) is simplified to:

$$\boldsymbol{H}^{n+1} = \boldsymbol{P} \cdot \left(\sum_{i=1}^{n_s} b_i \; \frac{\mathrm{d}}{\mathrm{d}\,\Delta\boldsymbol{\epsilon}_{n+1}} (\mathbf{k}_i)\right) \tag{18}$$

The total derivative with respect to the strain increment of Equation (14) is required, which may be expressed as:

$$\frac{\mathrm{d}\boldsymbol{k}_i}{\mathrm{d}\,\Delta\boldsymbol{\epsilon}_{n+1}} = \frac{\mathrm{d}\,\boldsymbol{F}\left(\boldsymbol{\Sigma}^{n} + \sum_{j=1}^{j<i} a_{ij}\mathbf{k}_j, \; \Delta\boldsymbol{\epsilon}_{n+1}\right)}{\mathrm{d}\,\Delta\boldsymbol{\epsilon}_{n+1}} = \tag{19}$$
$$= \frac{\partial\,\boldsymbol{F}_i}{\partial\,\boldsymbol{\Sigma}} \cdot \left[\sum_{j=1}^{j<i} a_{ij} \frac{\mathrm{d}\boldsymbol{k}_j}{\mathrm{d}\,\Delta\boldsymbol{\epsilon}_{n+1}}\right] + \frac{\partial\,\boldsymbol{F}_i}{\partial\,\Delta\boldsymbol{\epsilon}_{n+1}}$$

The terms of Equation (19) can be obtained as:

$$\frac{\partial\,\boldsymbol{F}_i}{\partial\,\boldsymbol{\Sigma}} = \frac{\partial\,\boldsymbol{F}\left(\boldsymbol{\Sigma}^{n} + \sum_{j=1}^{j<i} a_{ij}\mathbf{k}_j, \; \Delta\,\boldsymbol{\epsilon}_{n+1}\right)}{\partial\,\boldsymbol{\Sigma}} = \tag{20}$$
$$= \frac{\partial}{\partial\,\boldsymbol{\Sigma}}\left[\boldsymbol{\Psi}\left(\boldsymbol{\Sigma}^{n} + \sum_{j=1}^{j<i} a_{ij} \, \mathbf{k}_j\right) \cdot \Delta\boldsymbol{\epsilon}_{n+1}\right]$$

$$\frac{\partial\,\boldsymbol{F}_i}{\partial\Delta\boldsymbol{\epsilon}_{n+1}} = \frac{\partial\,\boldsymbol{F}\left(\boldsymbol{\Sigma}^{n} + \sum_{j=1}^{j<i} a_{ij}\mathbf{k}_j, \; \Delta\boldsymbol{\epsilon}_{n+1}\right)}{\partial\,\Delta\boldsymbol{\epsilon}_{n+1}} = \tag{21}$$
$$= \boldsymbol{\Psi}\left(\boldsymbol{\Sigma}^{n} + \sum_{j=1}^{j<i} a_{ij} \, \mathbf{k}_j\right)$$

Equations (18) to (21) define the consistent linearization of the explicit Runge-Kutta integration of a single strain increment in elastic or elasto-plastic regime, Equations (13) and (14). To evaluate the consistent linearization of the stress integration technique, the computation of the derivative of the product of the generalized stiffness matrix times the strain increment with respect to the generalized stress is required, Equation (19). This derivative is far more complex than the second order gradient of the plastic potential required in the linearization of implicit stress integration techniques. In this work, two different strategies have been followed for the computation of this term: (i) symbolic computations and (ii) numerical differentiation.

The methodology used to obtain the consistent tangent operator in the case in which only a single strain

increment in either elastic or elasto-plastic regime can be further extended to cope with all the situations of the general Sloan et al. (2001) algorithm. Expressions for all these other situations (correction of the yield surface drift, substepping, and elastic and elasto-plastic regime in a single strain increment) can be found in Monforte and Rouainia (2023).

5 REPRESENTATIVE NUMERICAL SIMULATIONS

This section reports a set of numerical simulations to assess the performance of the newly developed consistent tangent operator. After briefly describing the adopted constitutive model, the Modified Cam Clay model, results of the numerical simulation of an element test and a boundary value problem are presented.

The methodology reported in this work has been implemented in Matlab and the codes are openly available in a GitHub repository (Monforte and Rouainia, 2022).

5.1 Modified Cam Clay model

The Modified Cam Clay model has been chosen to assess the developed algorithms. As customary, the elastic response is described with a hypo-elastic model in which the bulk and shear modulus depend linearly on the mean effective stress:

$$K = \frac{p'}{\kappa^\star} \qquad G = \frac{3\,K\,(1-2\nu)}{2(1+\nu)} \tag{22}$$

where K and G are the bulk and shear modulus, ν is Poisson's ratio and p' is the mean effective stress. The parameter $\kappa^\star$ is the slope of the swelling line in the volumetric strain – logarithm of mean stress plane. The yield surface is expressed as:

$$f = \left(\frac{\sqrt{3\,J_2}}{M}\right)^2 + (p' - p_0)^2 - (p_0)^2 \tag{23}$$

where J_2 is the second invariant of the stress tensor and M is the slope of the Critical State line. The plastic internal variable, p_0, is equal to half of the pre-consolidation pressure, and varies with volumetric plastic strain, ϵ_v^p, as:

$$\dot{p_0} = \frac{p_0}{\lambda^\star - \kappa^\star}\,\dot{\epsilon_v^p} \tag{24}$$

where $\lambda^\star$ is the slope of the isotropic compression line in the volumetric strain – logarithm of mean effective stress plane.

Therefore, this model only has one internal variable, and the generalized stress is defined as:

$$\boldsymbol{\Sigma} = [\boldsymbol{\sigma},\ p_0] \tag{25}$$

5.2 Element test

The first numerical analysis of this work corresponds to an element test (i.e. only one Gauss point is considered), namely a drained triaxial loaded in compression. The adopted material parameters are representative of a soft clay: $\kappa^\star = 0.01$, $\lambda^\star = 0.1$, $M = 1$ and $\nu = 0.3$. Normally consolidated conditions are assumed.

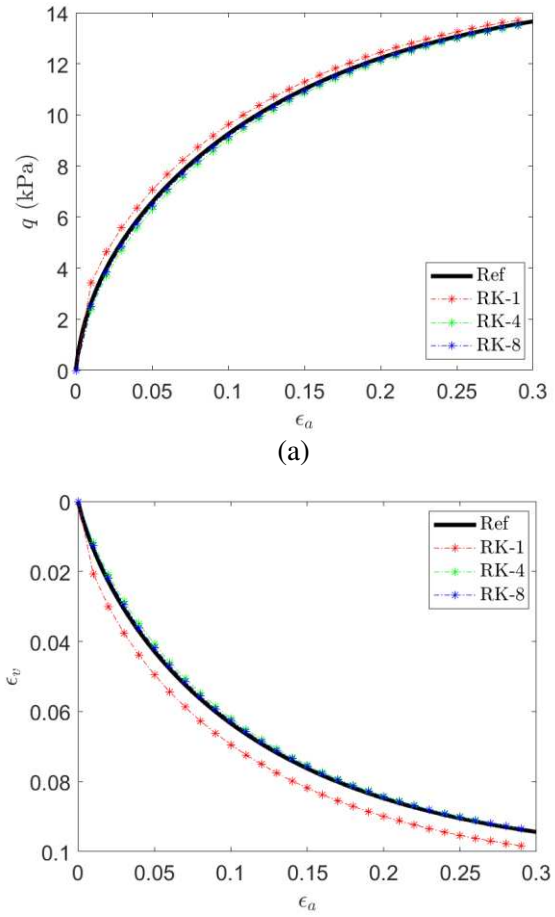

Figure 1. Drained triaxial test with different Runge-Kutta methods. (a) stress strain response and (b) volumetric response in terms of the axial strain.

Figure 1 reports the main output of interest of the test: the evolution of deviatoric stress, q, and volumetric strain, ϵ_v, in terms of the axial strain, ϵ_a. This problem has been computed with first, fourth and eighth order Runge-Kutta methods. Additionally, another simulation has been performed using a much higher number of load steps with an eighth order Runge-Kutta method (Reference solution). All numerical solutions show good agreement with the reference one, and that computed with the first order method has a larger error.

Drained triaxial loading has a mixed stress-strain control, so a non-linear system of equations must be solved for each loading step. This system of equations is solved using a Newton-Raphson method, and the Jacobian matrix involves terms related to the stiffness matrix.

Figure 2 compares the evolution of the norm of the residual in terms of the iteration number during the first loading step. If the consistent tangent operator is considered in the Jacobian matrix, the rate of convergence of the non-linear solver is quadratic, and only six iterations are required to achieve a norm lower than the specified tolerance. In contrast, by using the continuous stiffness matrix, the convergence rate is linear, thus the norm of residual decreases at a much lower pace with up to 78 iterations needed to reduce the norm of the residual below the tolerance.

This analysis confirms the correctness of the newly developed consistent tangent operator, which leads to a quadratic convergence rate. On the contrary, a linear convergence rate is obtained using a continuum stiffness matrix.

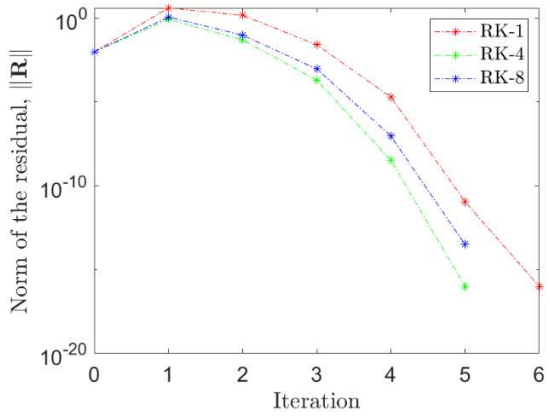

(a)

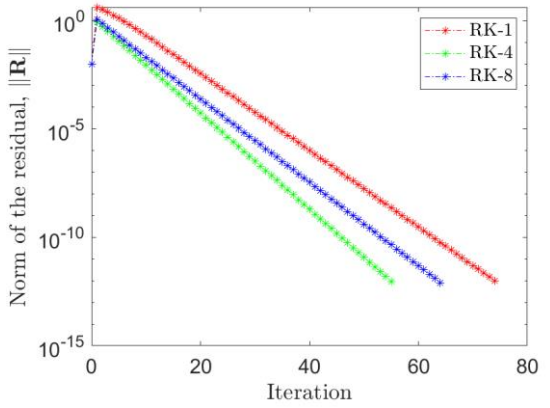

(b)

Figure 2. Drained triaxial test with different Runge-Kutta methods: norm of the residual during the first loading step. (a) Consistent tangent operator and (b) continuum stiffness matrix.

5.3 Boundary value problem

To further illustrate the performance of the newly developed consistent tangent operator, a boundary value problem is presented. A biaxial test is solved employing the finite element method, using the discretization presented in Figure 3(a). The sample has a height of 0.2 m and a width of 0.1m. An implicit time marching scheme is used in the global problem, and the resulting non-linear system of equations is solved with the Newton-Raphson method. The same constitutive parameters in the previous section are considered.

The initial stress state is characterized with horizontal and vertical effective stress equal to 10 kPa. Null displacements are prescribed at the bottom boundary, whereas null horizontal displacements and a downward movement are prescribed at the top boundary. At both vertical boundaries a constant horizontal load of 10 kPa is prescribed.

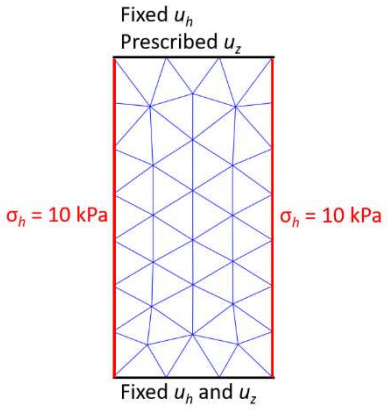

(a)

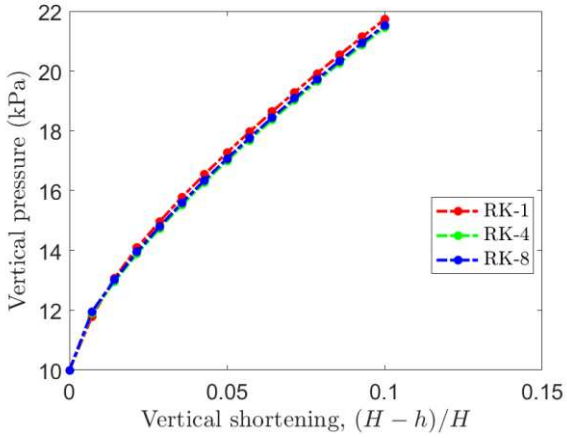

(b)

Figure 3. Biaxial test. (a)Finite element discretization, and (b) Load-displacement curve.

Figure 3(b) reports the load displacement curve computed using several Runge-Kutta methods. The solution obtained by all methods is comparable, but that obtained with the first order method presents a slightly stiffer response.

Again, to assess the performance of the newly developed consistent tangent operator, the same problem has been computed for the three Runge-Kutta methods utilising the consistent and continuum stiffness matrix in the nonlinear solver. Figure 4 reports the evolution of the norm of the residual in terms of the number of iterations during the first loading step. Convergence is achieved in less than nine iterations if the consistent tangent stiffness matrix is used, and the rate of convergence

of the iterative solver is quadratic. On the contrary, convergence is not achieved after 30 iterations using the continuum stiffness matrix and the rate of convergence is linear.

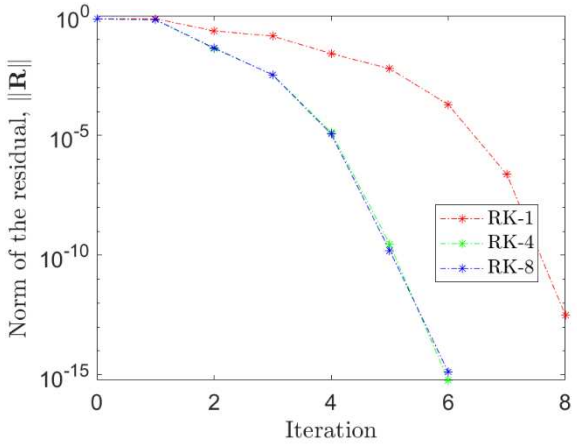

(a)

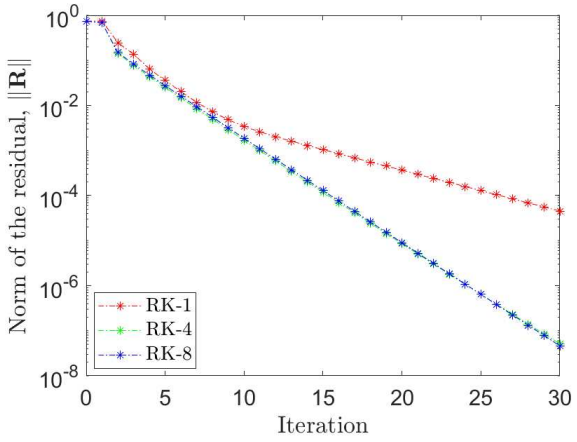

(b)

Figure 4. Biaxial test with different Runge-Kutta methods: norm of the residual during the first loading step. (a) Consistent tangent operator and (b) continuum stiffness matrix.

6 CONCLUSIONS

An expression for the consistent tangent operator of explicit, Runge-Kutta based stress integration techniques for elasto-plastic models has been proposed. In this work, only the case in which the strain increment results in the elastic regime or elasto-plastic regime have been considered, but the formulation can be extended to consider substepping, yield surface drift correction and cases in which the strain increment results in elastic straining followed by plastic flow (Monforte and Rouainia 2023).

The expression of the consistent linearization has been assessed in two numerical analyses, an element test and a boundary value problem, employing the Modified Cam Clay model. It has been shown that the proposed consistent tangent operator always renders a second order of quadratic convergence rate of the non-linear solver; instead, using the continuum stiffness matrix leads to a linear convergence rate. The use of the proposed expression for the consistent tangent operator improves the computational efficiency of explicit stress integration techniques. By implementing this expression, the use of accurate, high order stress integration schemes no longer comes at the cost of a much larger computational burden.

7 ACKNOWLEDGEMENTS

The first author acknowledges financial support of Ministerio de Ciencia e Innovación of Spain (MCIN/AEI/10.13039/501100011033) thorugh the Severo Ochoa Centre of Excellence project (CEX2018-000797-S) and research project PID2020-119598RB-I00. Support from the EPSRC Programme Grant ACHILLES (EP/R034575/1) is also acknowledged.

8 REFERENCES

Armero, F., Pérez-Foguet, A. 2002. On the forumulation of closest-point projection algorithms in elasto-plasticity – Part I: The variational structure. *International Journal for Numerical Methods in Engineering*, **53**(2), 297-329.

Borja, R. I. 1989. Linearization of elasto-plastic consolidation equations. *Engineering computations*, **9**, 163-168.

Lloret-Cabot, M., Sheng, D. 2022. Assessing the accuracy and efficiency of different order implicit and explicit integration schemes. *Computers and Geotechnics*, **141**, 104531.

Monforte, L., Rouainia, M. 2022. Consistent tangent operator for Runge-Kutta based explicit stress integration techniques for elasto-plastic models. Matlab implementation. https://github.com/lluis-mv/ExplicitStressIntegration

Monforte, L., Rouainia, M. 2023. A new consistent tangent operator for Runge-Kutta based explicit stress integration techniques for elasto-plastic models. *In preparation.*

Oliver, J., Huespe, A.E., Cante, J.C. 2008. An implicit/explicit integration scheme to increase computability of nonlinear material and contact/friction problems. *Computer Methods in Applied Mechanics and Engineering,* **197**(21), 1865-1889.

Pérez-Foguet, A., Rodríguez-Ferran, A., Huerta, A. 2001 Consistent tangent matrices for substepping schemes. *Computer Methods in Applied Mechanics and Engineering,* **190**(35-36), 4627-4647.

Rouainia, M., Muir Wood, D. 2001. Implicit numerical integration for kinematic hardening soil plasticity models. *International Journal for Numerical and Analytical Methods in Geomechanics,* **25**(13), 1305-1325.

Simo, J.C. 1998, *Numerical analysis and simulation of plasticity*. Handbook of numerical analysis. Volume 6. Elsevier.

Simo J.C., Hughes. T.J.R. 1998 *Computational inelasticity*. Springer.

Sloan, S.W., Abbo, A.J., Sheng. D. 2001. Refined explicit integration of elastoplastic models with automatic error control. *Engineering Computations*, **18**(1-2), 121-194.